NTNU – Trondheim
Norwegian University of
Science and Technology

Estimating seabed velocities from normal modes

Ole Wostryck Eiesland

Earth Sciences and Petroleum Engineering
Submission date: June 2012
Supervisor: Martin Landrø, IPT

Norwegian University of Science and Technology
Department of Petroleum Engineering and Applied Geophysics

Summary: In this Master Thesis a method for estimating seabed p-wave velocities from normal mode seismic data is developed. This is done through forward modeling using two dimensional finite difference modeling to generate synthetic data based on a given parallel two layered laterally varying seabed velocity model and a constant two layered density model, with a common fixed water depth. A semblance inversion technique is developed in MATLAB using the period equation (1) and the resulting velocity profiles is plotted against the exact velocity model to check the validity of the estimates. The same method is extended to estimations of seabed densities. For analysis of the robustness of the method, analysis with added pseudo random noise is preformed.

The results shows a good performance of the semblance method to reproduce the model velocity parameters. The introduction of noise is handled well and decent results are obtained for significantly low signal to noise ratios.

It suggests that the semblance method is applicable to use for determination of other parameters influencing the normal mode response signal.

Sammendrag: I denne master oppgaven utvikles en metode for å estimere p-bølge hastigheter i havbunnen. Dette gjøres gjennom fremover modellering ved bruk av todimensjonal endelig differanse modellering for å generere syntetiske data basert på en gitt parallell to lags lateralt varierende havbunnhastighetsmodell og en konstant to lags tetthetsmodell med felles havdyp. En semblance inversjons teknikk blir utviklet i MATLAB ved hjelp av periode ligningen (1) og de resulterende hastighetsprofilene blir plottet mot den eksakte hastighetsmodellen for å vise validiteten av estimatene. Den samme metoden blir utvidet til å estimere havbunnstettheter. For å undersøke hvor robust metoden er, utføres en analyse med tillagt pseudo tilfeldig støy.

Resultatene viser at semblance metoden presterer godt når den gjenskaper modelleringshastighetsparametrene. Introduksjon av støy håndteres godt og brukbare resultater oppnås for signifikante lave signal til støy forhold.

Det foreslås at semblance metoden kan benyttes til å bestemme andre parametre som innvirker på normal mode signalet.

Contents

1 Introduction

The theory of normal modes to describe the response of a acoustic source in the water layer is well known among different disciplines (oceanography, earthquake seismology, naval warfare) but not popularly used in exploration seismology.

At large source-receiver offsets the dominant recorded signal is reflections from within the water layer and refractions traveling on the interface between the water layer and the seabed. This signal is often called normal modes. In a paper by M. Landrø and P. Hatchell [3] it is suggested that lateral variations in velocity could be estimated by looking on the normal mode response.

This thesis sets forth to model the normal mode response and derive a method to estimate the lateral velocity variation in the seabed based on the modeled data.

Thanks to Prof. Martin Landrø for supervision on this project.

2 Theory

2.1 Normal modes

When a wave propagates in a two layered half space, e.g. water column overlaying sediment, the recorded signal at large horizontal distances from the source can be viewed as superimposed harmonic waves with different modes. In a text book by Ewing, Jardetsky and Press [2] the far field recorded signal from a source in the water layer is derived in detail. The following periodic equation (for acoustic case) can be used in the analysis of the signal recorded at large horizontal offsets.

$$\tan kH\sqrt{\frac{c^2}{\alpha_1^2}-1} = -\frac{\rho_2\sqrt{\frac{c^2}{\alpha_1^2}-1}}{\rho_1\sqrt{1-\frac{c^2}{\alpha_2^2}}} \tag{1}$$

In the equation, α_1 and α_2 is the P-wave velocity of the layers above and belove the seabed respectively, ρ_1 and ρ_2 is the density of the upper and lover layers respectively, k denotes the wavenumber, H is the water depth and c is the phase velocity.

It exists a relation between the phase-, c, and the group velocity, U, with respect to frequency. c could be determined from equation (1) and U equals the derivative of angular frequency with respect to wave number [2, 3]. A plot of these curves, also called dispersion curves, for a model with $\alpha_2 > \alpha_1$ and $\rho_2 > \rho_1$ can be seen in figure 1 taken from M. Landrø and P. Hatchell (2011) [3].

As the velocity parameters of the subsurface changes, a shift in the dispersion curves is observed (figure 2). The shift is more subtile for smaller parameter contrasts and larger for velocity change than for a change in the density ratio (figure 3).

2.2 Real data example

Figure 4 shows real life of field seismic data acquired on the Valhall field in the north sea. The data is 4C, from buried seismic cables. Analysis is done by Landrø and Hatchell [3]. The data clearly shows multiple modes and an attempt to fit theoretical dispersion curves to the data. Validity of the fit is limited due to the simplified assumption of a two layered medium (curve overlay).

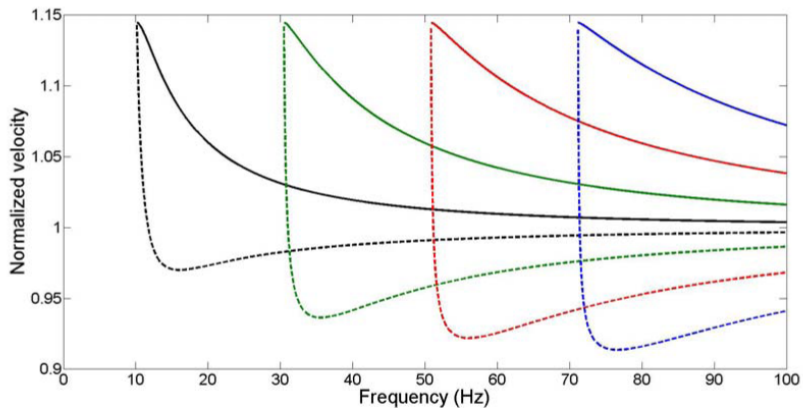

Figure 1: Dispersion curves for a two layered medium for the first four modes. $\alpha_2 > \alpha_1$ and $\rho_2 > \rho_1$. c is solid line, U is dotted line. Figure by M. Landrø and P. Hatchell (2011) [3]

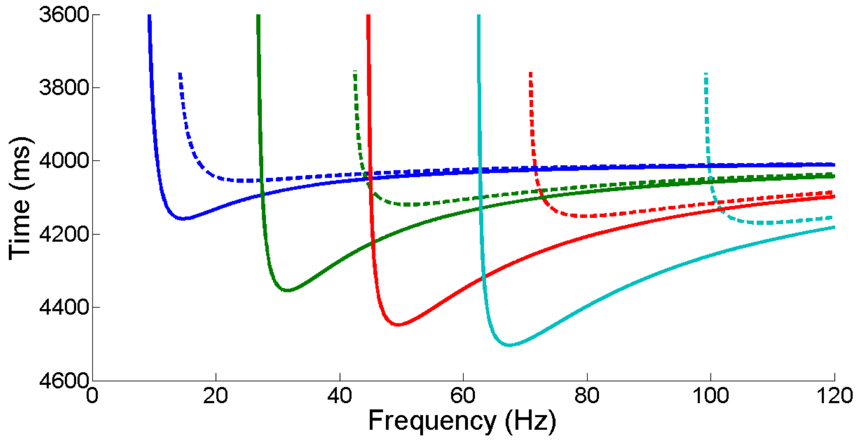

Figure 2: The effect of different α_2 values on group velocity dispersion curves for a two layered medium for the first four modes. Solid line is $\alpha_2 = 1800m/s$ and dotted line is $\alpha_2 = 1600m/s$. $\alpha_1 = 1500m/s$ and $\frac{\rho_2}{\rho_1} = 1.6$ for both cases. Water depth, $H = 76m$.

3 Method

3.1 The model

The environment model used to compare the two methods is shown in figures 5 and 6, where the offset $x = 6000m$, $H = 76m$, $\alpha_1 = 1500m/s$, $\rho_1 = 1000kg/m^3$, $\alpha_2 = 1800 - 1600m/s$ and $\rho_2 = 1600kg/m^3$. The top layer

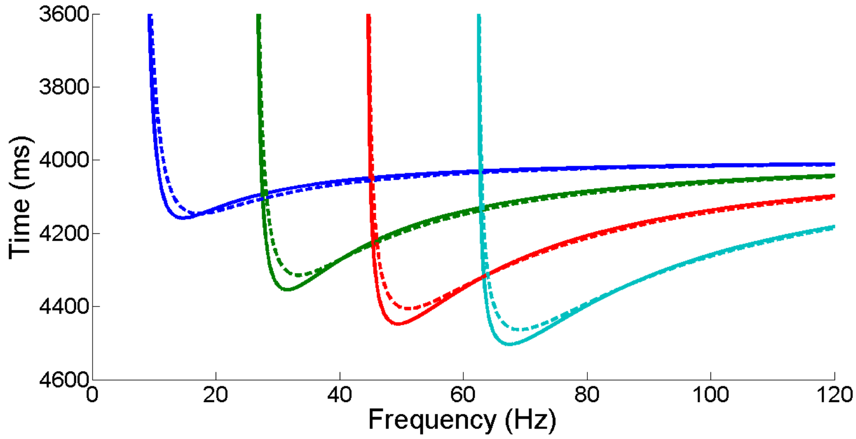

Figure 3: The effect of different $\frac{\rho_2}{\rho_1}$ values on group velocity dispersion curves for a two layered medium for the first four modes. Solid line is $\frac{\rho_2}{\rho_1} = 1.6$ and dotted line is $\frac{\rho_2}{\rho_1} = 1.2$. $\alpha_1 = 1500m/s$ and $\alpha_2 = 1800m/s$ for both cases. Water depth, $H = 76m$.

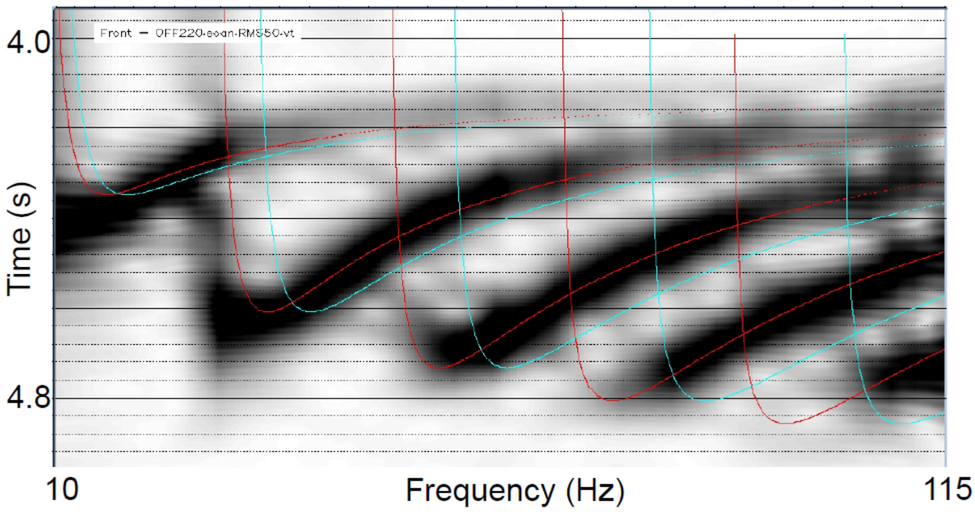

Figure 4: Real data from the Valhall field. Figure by Landrø and Hatchell. [3]

represents the sea limited above by a free surface and a downward unlimited bottom layer. The area of interest in the model is where α_2 over an area of five kilometers linearly changes from left to right from $\alpha_2 = 1800m/s$ to $\alpha_2 = 1600m/s$. See figure 6.

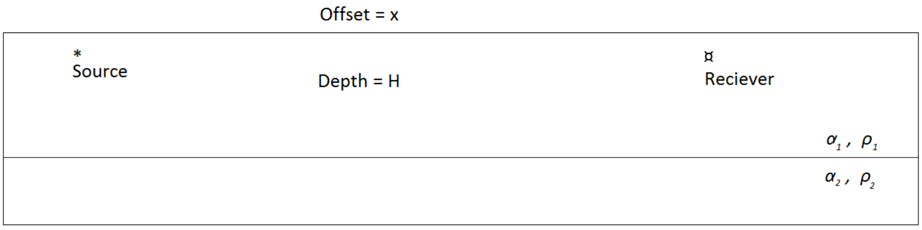

Figure 5: Sketch of model used. $x = 6000m$, $H = 76m$, $\alpha_1 = 1500m/s$, $\rho_1 = 1000kg/m^3$, $\alpha_2 = 1800 - 1600m/s$ and $\rho_2 = 1600kg/m^3$

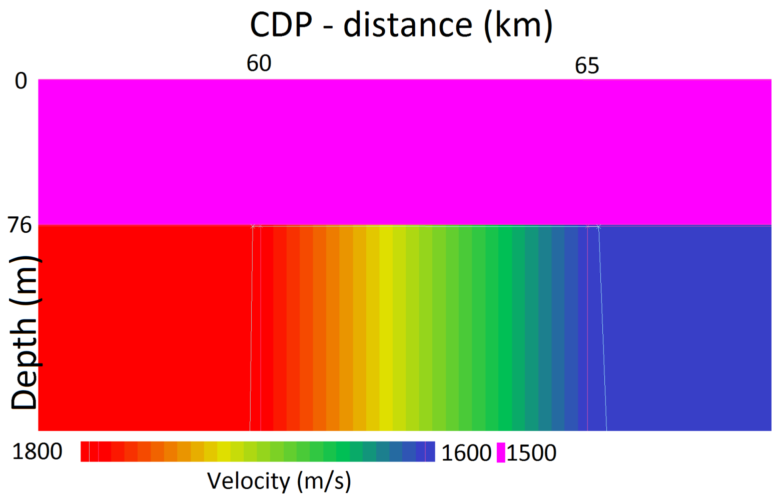

Figure 6: Color coded velocity model

3.2 Finite difference

One of the methods proven to be most successful in simulating seismic surveys is a numerical solution method of the differential wave equations called finite difference modeling [4]. In essence this powerful method uses a grid containing points with the values of the physical parameters, e.g. velocities and densities, of the medium the waves are propagating through and expresses the wave equations in the time domain to solve it recursively in time steps. Initial conditions are zero particle and stress fields. Before modeling the boundary conditions is specified, typically the choice of free surface or not at the model top (i.e. Multiples or not). The left, right and bottom boundaries are in most cases unbounded i.e. modeled as absorbing.

Since the solutions of the wave equations is numerical, approximation errors are known to exist. Choosing appropriate modeling parameters is the key to success. The method is discrete so errors can propagate from time step to time step and magnify. Equation (2) shows the stability criteria to minimize errors, where Δt is the time sampling interval, Δx is the space sampling interval and V_{max} is the maximum velocity in the model.

$$\Delta t < 0.606 \frac{\Delta x}{V_{max}} \tag{2}$$

Combating these errors and obtain good quality data at minimum CPU time is a balance that should be kept in mind during the process of grid design.

Another error is grid dispersion which happens when spatial derivatives is truncated. Depending on the precision of the method a minimum of grid points per wavelength should be specified.

In this project the results are produced with the Promax seismic software package by Landmark. The Promax FD-code is a 4th order stencil driven acoustic 2D finite difference program. The program is derived from one developed by John Vidale at the Seismological Lab of the California Institute of Technology. The Promax code is well tested and should produce reliable results.

This finite difference method is two dimensional propagation, an as a result the wave form is different from a wave propagating in three dimensions. This will affect the magnitudes of the amplitudes only, and will not affect the phase of the wave [9]. When looking at the results, please keep this in mind.

3.3 Processing

3.3.1 Dispersion Display

In order to compare the dispersion of the modeled trace with the predicted dispersion curves of the period equation (1) some processing is necessary. Based on the method from [3]; The single trace for the desired offset is filtered with a narrow ($10Hz$ wide with slope width of $3Hz$) sliding bandpass filter. The result is an ensemble of traces showing amplitudes and their arrival times of the different frequency components of the original trace. Then a sliding RMS window function smoothed the data.

3.3.2 Semblance

Semblance 1 A common method to determine the similarity of a theoretical case and experimental data is the semblance plot [8]. In this case the starting point is the dispersion curves produced by the period equation (1). A Period equation (1) MATLAB script by M. Landrø was modified so that the dispersion curve samples fitted the data samples of the modeled dispersion displayed trace. The amplitudes of the corresponding time and frequency of the theoretical dispersion curves in the modeled dispersion data was summed for all visible modes, and repeated for different values of α_2 and ρ_2.

$$S_n = \sum_{m=1}^{4} \sum_{\rho=\rho_{2,start}}^{\rho_{2,end}} \sum_{\alpha=\alpha_{2,start}}^{\alpha_{2,end}} \sum_{i=1}^{n} D(d_{m,\alpha,\rho}(f_i), f_i) \tag{3}$$

Equation (3): $D(t, f)$ is the amplitude as a function of travel time, t, and frequency, f. $d_{m,\alpha,\rho}(f_i)$ is the travel time for mode m for each sample value of α_2 and ρ_2 as a function of f. n is the maximum frequency to sum.

Semblance 2 After looking at the results from the above mentioned approach to the semblance method, an effort was made to try to improve the robustness of the method. Taking the sample points from the first four modes presented by equation (1) a filtered normal mode response, $Sg(t, f)$, was produced by convolving a pulse, $p(t)$, with the traces, $r(t, f)$, consisting of the samples taken from the period equation (1). Equation (5)

The pulse, $p(t)$, used was chosen to resemble the filtered RMS finite difference modeled data, and is on the form of equation (4):

Figure 7 shows the result.

$$p(t) = e^{k(t-\tau)^2} \tag{4}$$

$$Sg(t,f) = (\sum_{m=1}^{4} r_m(t,f)) * p(t) \quad (5)$$

Equation (5): $Sg(t,f)$ is the amplitude as a function of travle time, t, and frequency, f. m is the mode number. $r_m(t,f)$ is a spike function of time and frequency corresponding to the sample points of the dispersion curves of the period equation (1), for any given parameters.

The above described convolution was preformed for every velocity and density value of interest and each trace multiplied with the corresponding trace from the finite difference filtered modeled response. The remaining sample values in the seismogram is summed as the semblance value for the particular velocity and density values.

Figure 8 shows a semblance plot of the method tested on the synthetic convolved filtered normal mode response, i.e on itself.

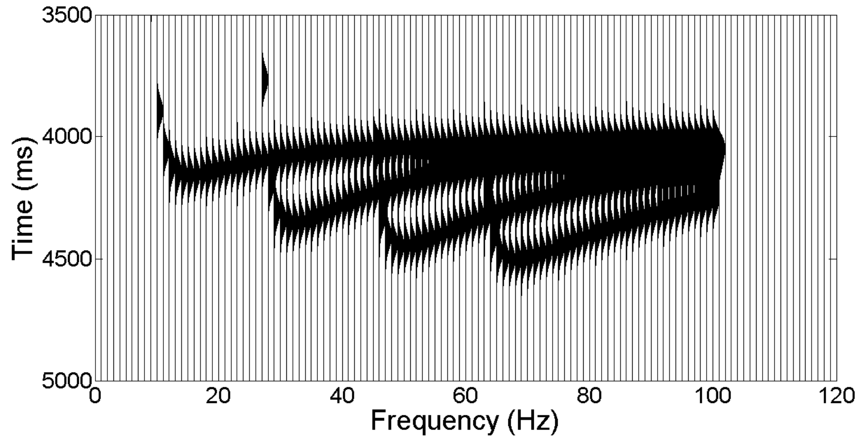

Figure 7: Synthetic convolved filtered normal mode response. Note the strong signal towards the "tail" as the curves converges. Using an frequency independent amplitude pulse in the convolution causes this. It is clearly erroneous compared with the modeled results (figure 12). The solution before semblance analysis is to apply a mute to the modeled data.

Testing showed strong noise influence and observing that the response from the "tail"-section of the synthetic convolved data (figure 7) was a mismatch, due to frequency independent amplitude of the convolved pulse, to the modeled data that contains most energy around the group velocity minimums and around $50Hz$. A muting tool script was written to isolate the normal mode response before multiplication and summation. Figure 9 shows

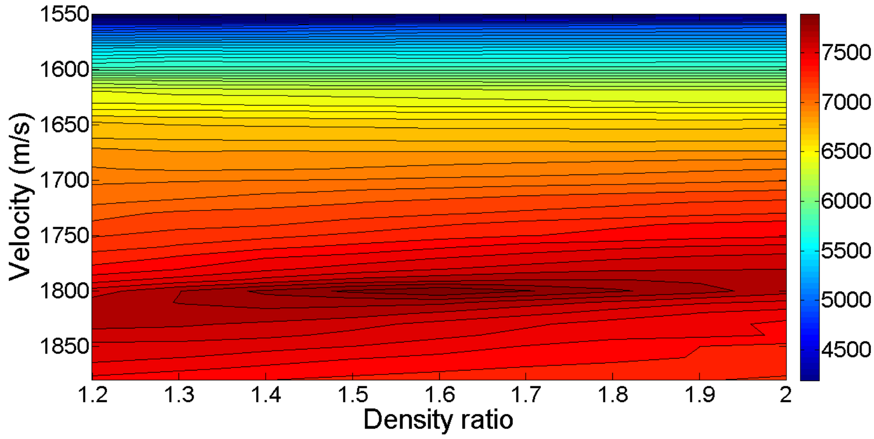

Figure 8: Semblance plot. Synthetic convolved filtered normal mode response. Model parameters are: α_2, y-axis, of $1800m/s$ and density ratio, x-axis, of 1.6.

the modeled dispersion curves after mute with the top and bottom mute lines drawn in.

4 Results

Velocity models and density models according to figure 5 and 6 was used as input to the modeling program. A $50Hz$ peak frequency ricker wavelet was used in the modeling. Next the source and receiver locations was specified. A total of 15 shots was modeled over the interval of the velocity change. The shot spacing was 1000 meters. A shot gather from the left side, CDP $57km$, $\alpha_2 = 1800m/s$, of the velocity anomaly is shown in figure 10.

A processing flow was created to select the trace at 6000 meters offset and export it as ascii data for further processing in MATLAB. Figure 11 shows a raw trace at 6000 meters offset from the gather displayed in figure 10.

The traces was then filtered as described in section 3.3.1 and the resulting dispersion display is showed in figure 12. Given the nature of the $50Hz$ peak frequency ricker wavelet the energy is concentrated around $50Hz$ making the first and fourth mode less pronounced. A slight frequency dependent gain function is applied in figure 12 to better display the first four modes.

Figures 13 and 14 shows the results for the CDP locations in the middle of the decreasing velocity zone, CDP 62, and after, CDP 68, with dispersion curves overlay calculated from equation (1) using the true model velocities and densities at the corresponding CDPs.

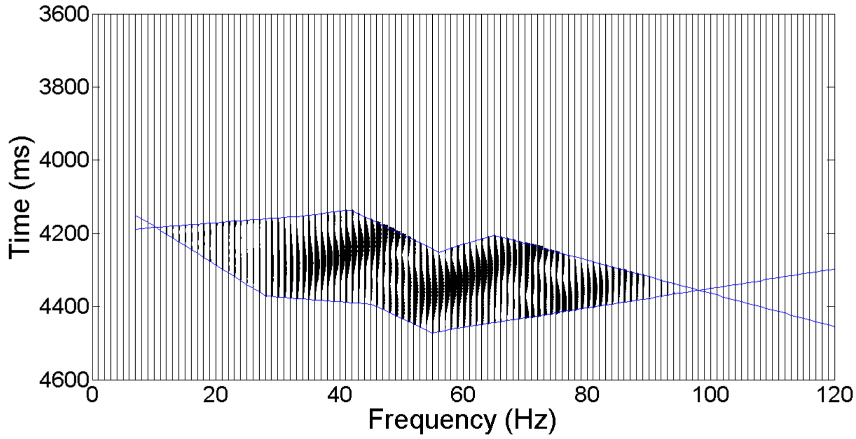

Figure 9: Dispersion curves after applied mute to remove noise and unwanted mismatch effect from proceeding semblance analysis. CDP $60km$

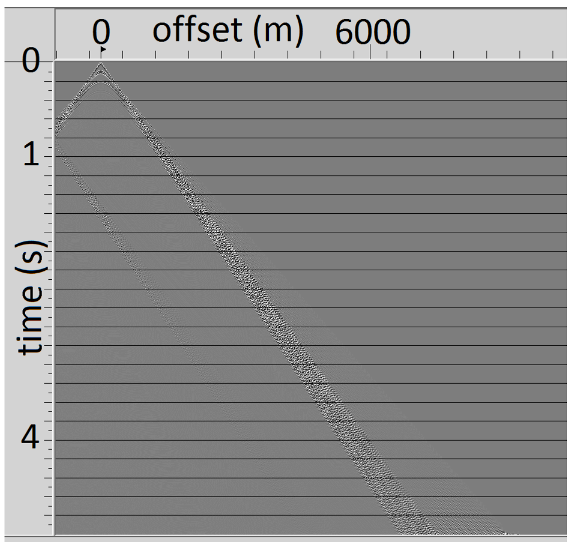

Figure 10: Gather display of finite difference simulated data. CDP $57km$

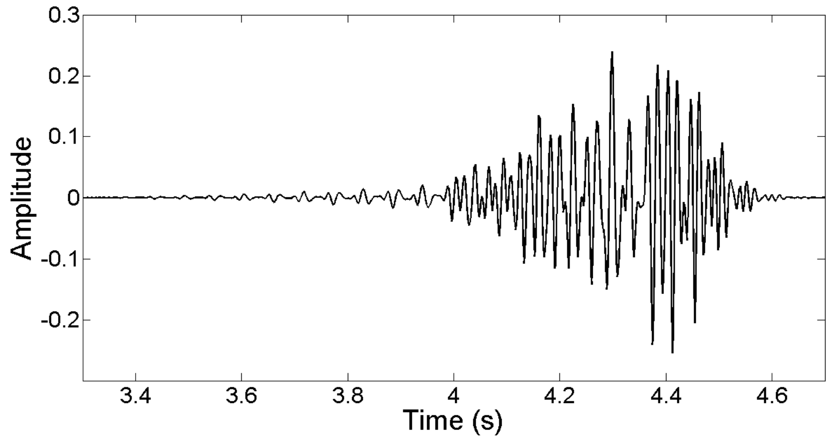

Figure 11: Raw trace from FD modeling. CDP $57km$

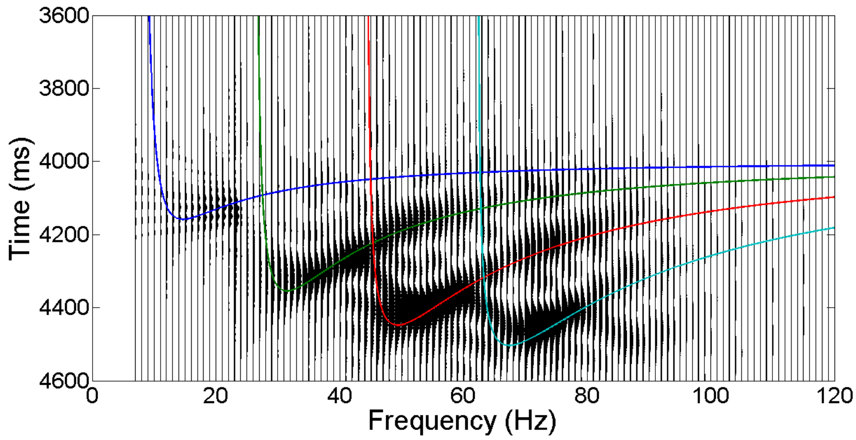

Figure 12: Dispersion curves. CDP $57km$

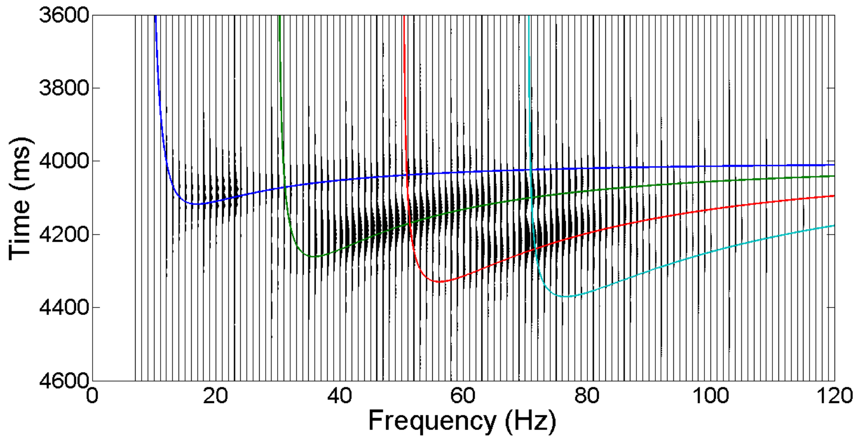

Figure 13: Dispersion curves. CDP 62km

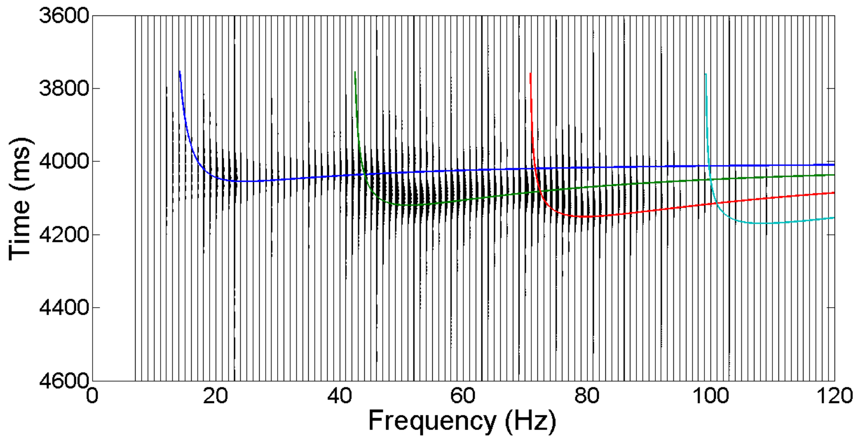

Figure 14: Dispersion curves. CDP 68km

From figure 12 with the help of the overlaid theoretical curves one can observe a reasonable good fit. This observation is especially true for the first two modes but the fit decreases for the last two i.e. with increasing frequency.

Finally the inversion algorithm based on the semblance method described in section 3.3.2 was applied to the data. Figures 15, 16 and 17 displays semblance plots for three traces of three shots with coverage near and over the interest zone. The plots shows a good sensitivity with respect to velocity change and, to less extent, a sensitivity to density variations. The plots are constructed using semblance method 1.

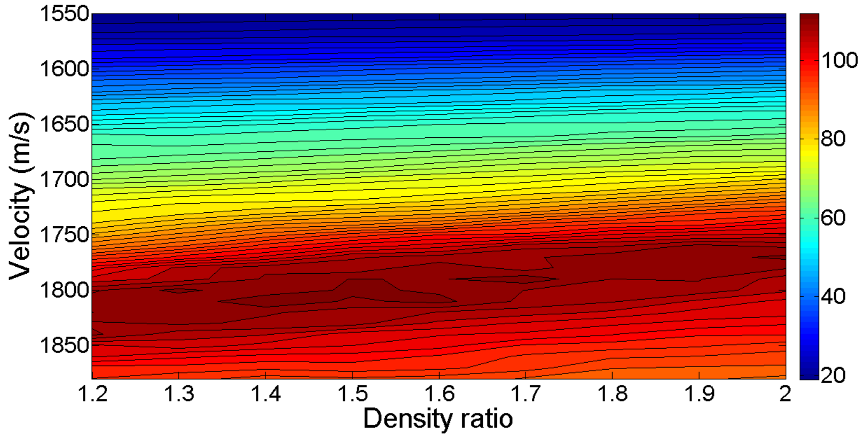

Figure 15: Semblance plot, method 1. CDP 57km

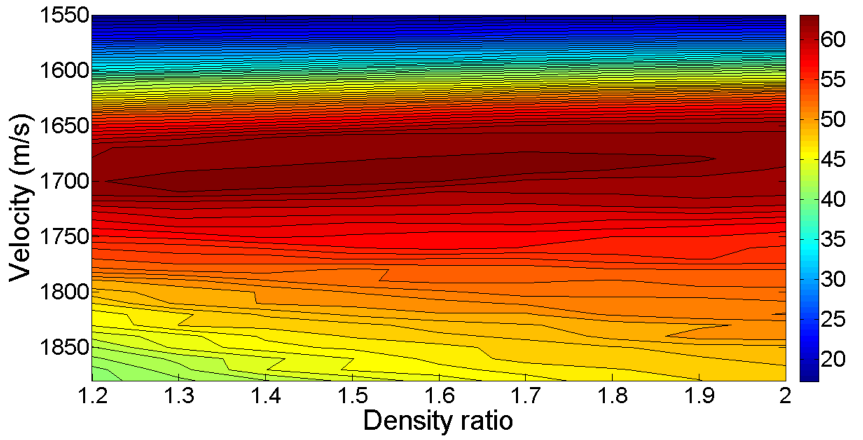

Figure 16: Semblance plot, method 1. CDP 63km

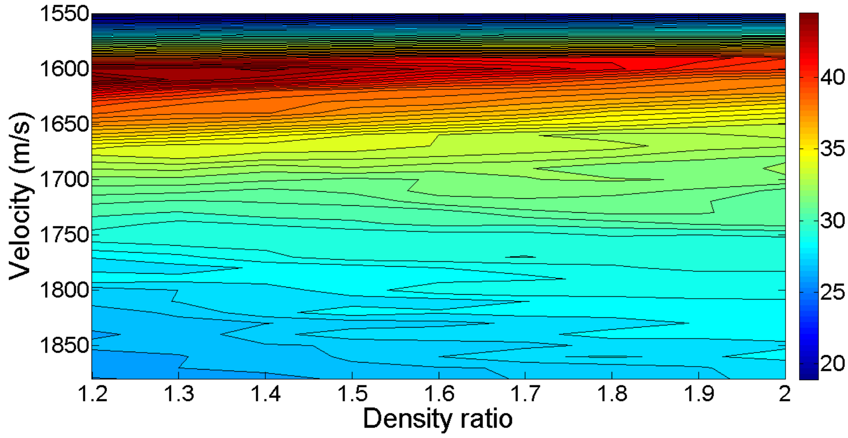

Figure 17: Semblance plot, method 1. CDP $68km$

Figure 18 shows the predicted velocities picked from the maximum semblance values for all fifteen shots versus CDP location. The red stippled line is the true velocity profile used in the modeling. The gradual decreasing trend is represented reasonably well and the deviation at a point is no more than $20m/s$ on average.

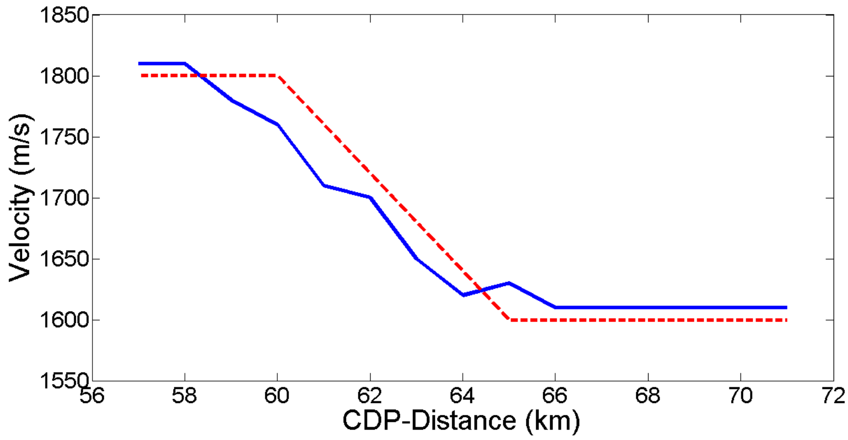

Figure 18: Velocity profile, semblance method 1

4.1 Noise

To study the robustness of the semblance method and its reliability, noise was added to the traces. The noise added was random both with respect to maximum amplitude of the shot and the shots/traces.

As seen in figures 20 and 19 with signal to noise ratios ($\frac{S}{N}$) of $\frac{1}{2}$ and 1 respectively it is hard to deduce anything at all from just looking at the raw data.

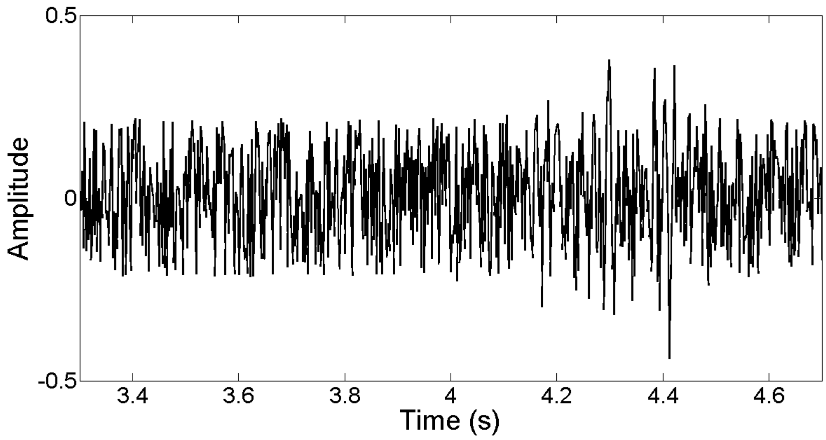

Figure 19: Rawtrace. $\frac{S}{N} = 1$

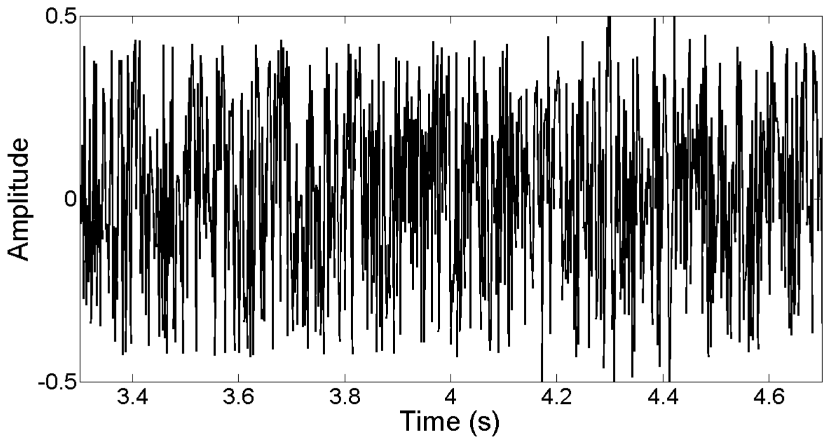

Figure 20: Rawtrace. $\frac{S}{N} = \frac{1}{2}$

After displaying the traces in the time-frequency domain it becomes clear that the dispersion curves for the $\frac{S}{N} = 1$ case (figure 21) is still reasonably well represented but the $\frac{S}{N} = \frac{1}{2}$ case (figure 22) is very contaminated, although the energy is visible it fits not so well to the theoretical curves. No gain was applied.

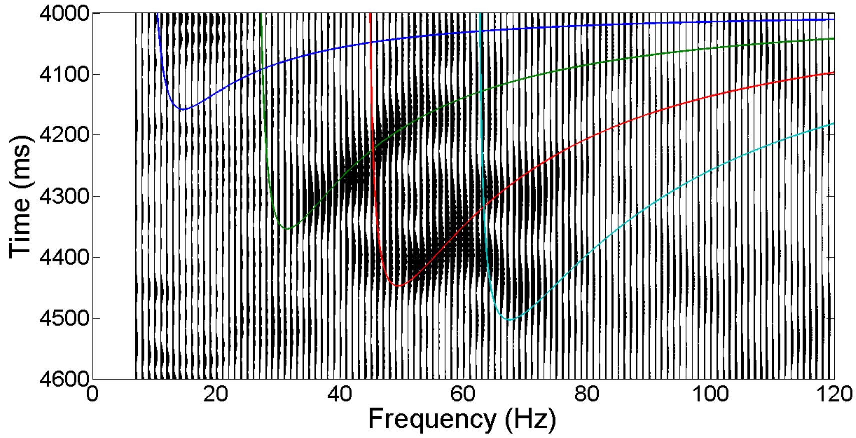

Figure 21: Dispersion curves. $\frac{S}{N} = 1$. CDP $57km$

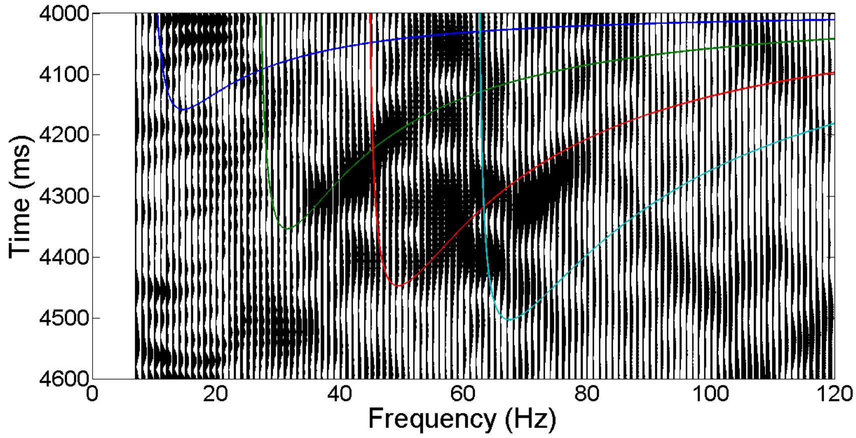

Figure 22: Dispersion curves. $\frac{S}{N} = \frac{1}{2}$. CDP $57km$

Applying the semblance inversion method 1 and looking at the resulting predicted velocity profiles, Figures 23 and 24 one can observe that the $\frac{S}{N} = 1$ case holds its shape quite good until it reaches lower velocities, while the $\frac{S}{N} = \frac{1}{2}$ case data is inconsistent and fluctuates more at low α_2 values.

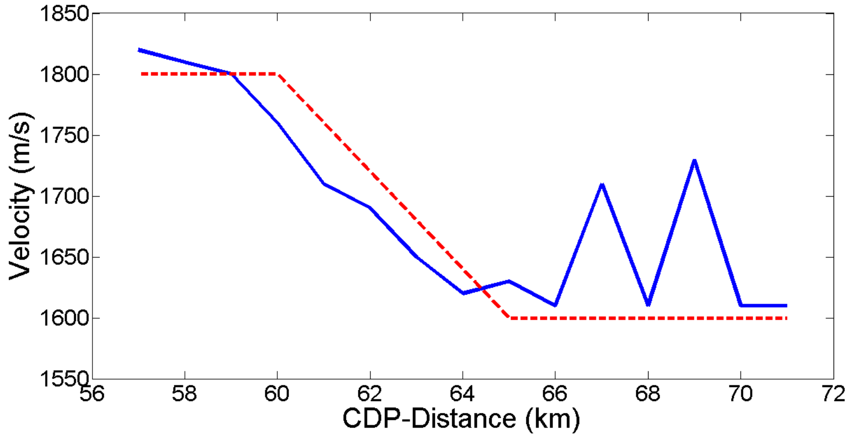

Figure 23: Velocity profile, method 1. $\frac{S}{N} = 1$

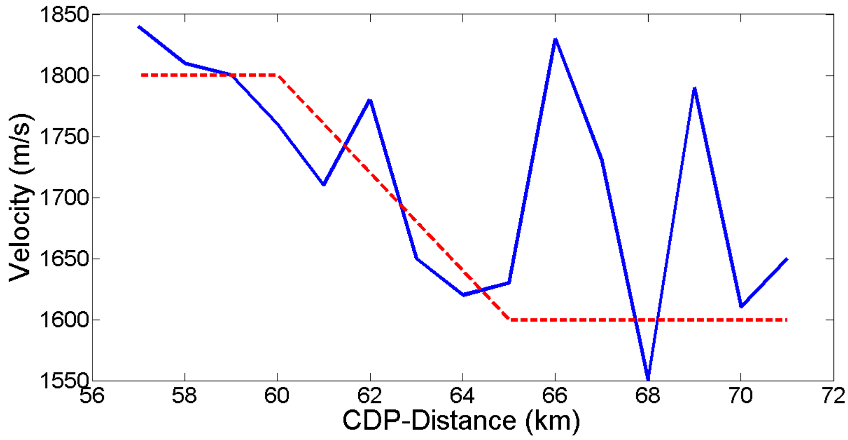

Figure 24: Velocity profile, method 1. $\frac{S}{N} = \frac{1}{2}$

The results form the same data as in figures 23 and 24 using the second semblance method are shown in figures 25 and 26. The key difference between the two methods is the muting, and provided that it is possible to distinguish the normal modes from the noise and apply a reasonable mute, the result is improved compared with method 1 for the $\frac{S}{N} = 1$ case (figure 25). For the $\frac{S}{N} = \frac{1}{2}$ case as seen in figure 22 the above mentioned problem starts to present. It is hard to distinguish the signal form the noise. What figure 26 shows is semblance method 2 with mutes based on the results obtained in method 1 (figure 24), assuming no major discontinuous jumps between shots. The result is surprisingly good. Certain mutes picked is based on interpretation and may be colored from knowledge of this particular dataset, and therefore should be considered as an absolute best case result.

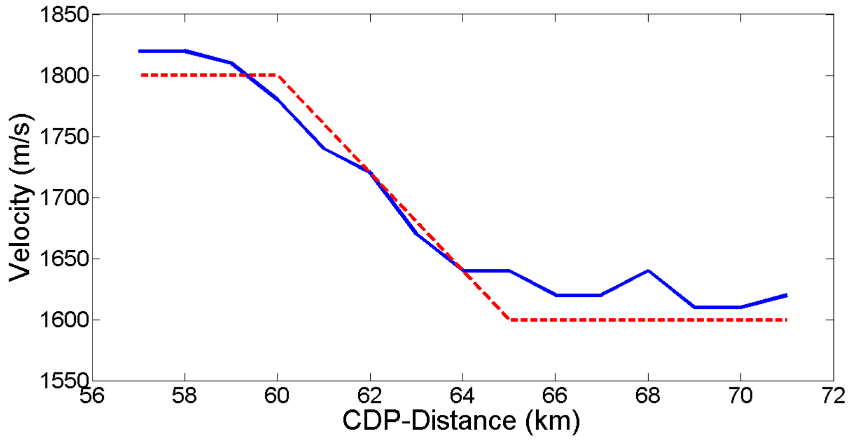

Figure 25: Velocity profile, semblance method 2. $\frac{S}{N} = 1$

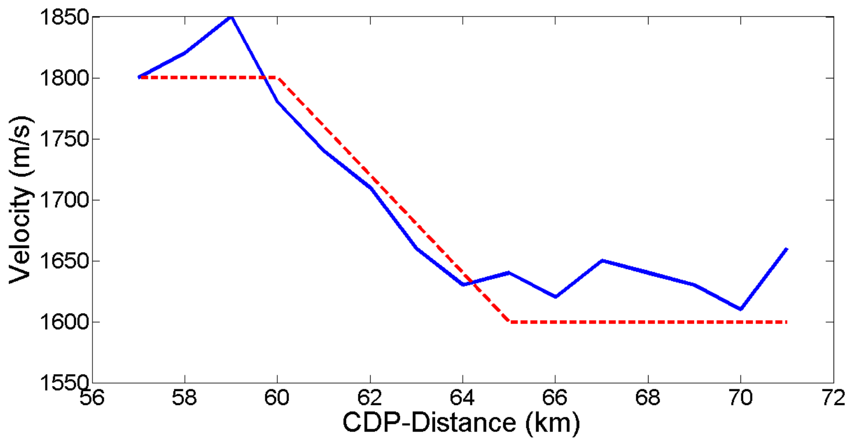

Figure 26: Velocity profile, semblance method 2. $\frac{S}{N} = \frac{1}{2}$

4.1.1 Densities

Incorporated in the semblance analysis tool was an attempt to recall the densities of the model environment. In figures 27 and 28 the resulting predicted density profiles, blue solid line, are plotted with the exact values used in the model, red dotted line.

The curve from method 1 (figure 27) shows quite erratic behavior while the curve from method 2 shows consistent density ratios versus distance of $\frac{\rho_2}{\rho_1} = 1.2$. Although the value is too low (exact $\frac{\rho_2}{\rho_1} = 1.6$), the consistency indicates an improvement for method 2 over method 1. An explanation for the low $\frac{\rho_2}{\rho_1}$ value is proposed in the discussion (section 5).

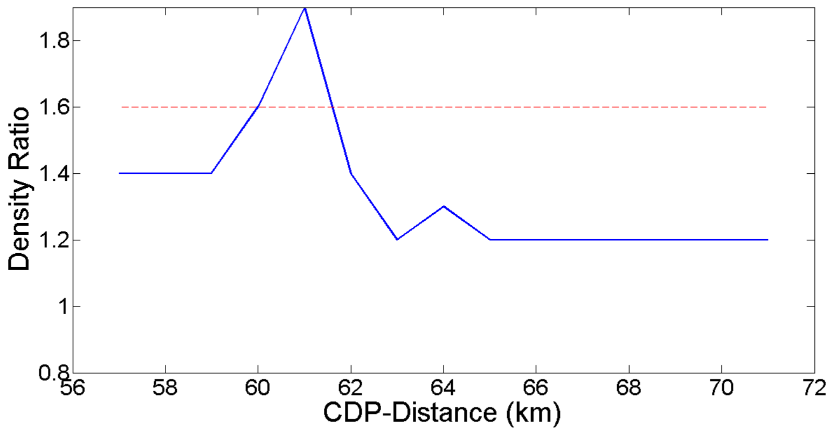

Figure 27: Density profile, semblance method 1. Noise free

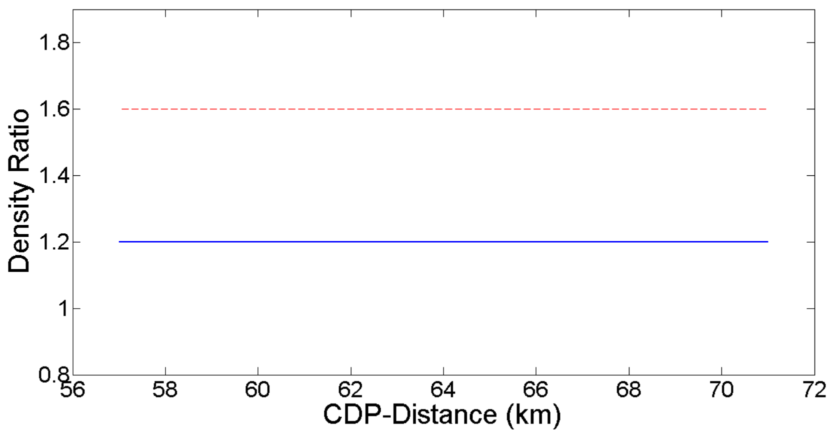

Figure 28: Density profile, semblance method 2. $\frac{S}{N} = \frac{1}{2}$

5 Discussion

As seen in the results, a few issues arise in the finite difference modeling of the normal mode response. The fit between the period equation (1) predicted dispersion curves and the time-frequency displayed finite difference modeled response is not exact and decreases with increasing frequency. This is to be expected, the higher frequencies is more subjected to numerical dispersion and as the figures shows, in accordance with numerical dispersion relations [8] the travel time shift is towards higher velocities (lower travel time). Grid size and time step length was minimized to counter this effect as much as possible (run time goes towards infinity) but was unable to completely dispose of the problem. For the same reason, theoretically predicted sample points do not coincide with modeled energy, the semblance predicted velocity profiles shows too high velocities.

For the same reason as discussed above, the density profiles produces by the semblance method shows too low density ratios. The theoretical dispersion curves in figure 3 shows the change in the dispersion curves when the density ratio goes from 1.6 to 1.2. The result is, in effect, to shift the group velocity minima towards faster travel times. Most of the energy is present around these group minima, therefore prediction errors in density ratios is likely to be caused by numerical dispersion form the finite difference modeling. The effect is more severe for the density ratio since the effect of changing the density ratio on the dispersion curves is small for reasonable sea bottom density ratios.

When the contrast between the water velocity α_1 and the sea bottom velocity α_2 becomes small, as on the right side of the model used in this modeling, the acoustic impedance contrast is reduced and the reflection coefficient is reduced [6] resulting in a weaker reflection from the sea bottom and less energy, weaker amplitude, is recorded at the receiver. Since the added noise is a function of maximum amplitude of each shot, the traces recorded over an area with low velocity contrast is more dominated by noise than shots recorded over an area with higher velocity contrast. As shown in the results this manifests in fluctuations in the low α_2-part (right part) of the noisy velocity profiles.

The modeling is done over a distance of $6000m$ and the units in the velocity profile is the mid point between the source and the receiver. The α_2 parameter is an average value over the $6000m$. The fact that the discrepancy in distance is not more pronounced, the opposite might be expected, is positive. A steeper linear reduction in velocity or a longer source-receiver offset will shift the kink point in the predicted velocity curve. By taking the last mid point with no change in velocity before the kink, and adding half the offset one should get close to the exact location of the lateral velocity change (accuracy of plus one shot distance). Similar for the second kink (subtract half offset, accuracy of minus one shot distance).

The simple horizontally plane two layered acoustic models used in the modeling of the data is a gross simplification compared to reality.

The sound speed in the water column is known to change with depth.

For consolidated second layers the shear wave velocity will influence the recorded signal. The period equation (1) for non-zero shear wave velocity [2] could be utilised in the semblance analysis and inversion provided the shear effect is not too small for the semblance resolution.

An other physical phenomenon that has been implemented in the period equation (1) is anisotropy [10]. The effect of anisotropy on the dispersion curves is small, but for a vertically transverse isotropic medium, extraction of the ϵ parameter is plausible.

For the case of a varying sea depth, provided it is continuous, could be compared with the varying velocity case. An average could be calculated, and should post no problem to this method. It is unlikely water depth data is not available.

In theory, for a two layer model, the semblance method should work for all cases, but interpretation is needed if parameters cause multiple semblance highs or the effect on the dispersion curves is small for small changes in a given parameter.

The acoustic finite difference modeling, lacking shear wave propagation, does not account for AVO (amplitude versus offset) effects but considering most reflections at such large offsets is post critical (and total) it is safe to neglect AVO.

Most of the amplitude is concentrated around the group minimum for each mode. This is observed in the modeled data and, to less extent, in the real data 4. This is partly the reason for the necessity of the mute, but as an phenomenon could be a significant property of the normal mode response in itself.

6 Conclusion

The results displays a good fit between the theoretical predictions and the modeled data. The semblance method developed to reproduce the α_2 velocity profile for the sea bottom produces reasonable results up to a signal to noise ratio between 1.0 and 0.5. The change in the dispersion curves for the different physical parameters dicides the sensitivity of the semblance method. The effects of velocity change is grater than that of density change, hench velocity change is easier to map. Soulutions for the normal mode response exists for a wealth of parameters, given a high enough resolution, semblance techniques should provide interesting data for analysis. Theoretical two layered model is a simplification, further studies is needed to check the validity of the methods in real seismic experiments.

References

[1] M. Landrø and L. Amundsen, *Using water layer normal modes to detect shallow gas and CO2 leakage*, (2011)

[2] Ewing, Jardetsky and Press,: *Elastic waves in layered media*, McGraw-Hill., (1957)

[3] M. Landrø and P. Hatchell: *Normal modes in seismic data - revisited.*, (2011)

[4] L. T. Ikelle and L. Amundsen: *Introduction to petroleum seismology*, Society Of Exploration Geophysicists., (2005)

[5] S. J. Laster, J. G. Foreman and A. F. Linville: *Theoretical investigation of modal seismograms for a layer over a half-space*, Geophysics, (1965)

[6] R. E. Sheriff and L. P. Geldart: *Exploration seismology - Extraction*, Cambridge University Press; 2 edition, (1995)

[7] CREWES: *Consortium for Research in Elastic Wave Exploration Seismology*, (http://www.crewes.org/ResearchLinks/FreeSoftware/), (2012)

[8] M. Landrø: *Seismic Processing and Imageing*, (NTNU), (2010)

[9] J. Helgesen: *Inversion of seismograms using finite difference modelling techniques*, (NTH), (1990)

[10] L. Skopintseva, M. Landrø and A. Stovas: *Normal modes in anisotropic VTI media*, (NTNU), (2012)

List of Figures